

Sébastien Dirren\*, Huw C. Davies  
 Institute for Atmospheric Sciences, ETH, Zurich, Switzerland

## 1. INTRODUCTION

Distinctive small amplitude perturbations of a baroclinic flow can yield transient growth rates beyond those of the system's normal modes (see e.g. Farrel, 1982), and this emphasizes the initial-value non-modal aspect of atmospheric development. One theoretical approach to this facet of development is the singular vector (SV) technique that yields the perturbations to a basic flow which amplify linearly most rapidly in a specified finite time period, for a prescribed norm. The approach is used in ensemble forecasts to analyse error growth (Molteni *et al.*, 1996).

Recent studies have sought to interpret the dynamics of SV perturbations. Badger and Hoskins (2000) investigated mechanisms by which finite time localized perturbation growth can occur and analysed the structure of the SV in simple models and in the ECMWF system. SV were found to grow initially by unshielding vertically compact structures and by untilting their westward-tilted structure by the zonal shear flow. Morgan (2000) used diagnostic techniques to understand SV development and found a SV evolution in three stages : unshielding, boundary-interior vorticities interaction and normal mode growth. SV theories point out that lower tropospheric perturbations are optimal for growth for long optimization times. Lower locations are favourable for inducing large amplitude signals at upper and lower levels that can then interact and co-develop. In contrast Fehlmann and Davies (1997) indicated that finite-amplitude upper-level potential vorticity (PV) anomalies can exert a strong influence upon surface cyclogenesis and error growth.

In the present study we examine the initial-value problem of baroclinic development in a potential vorticity framework and from a phenomenological standpoint. One paradigm for extratropical cyclogenesis is the approach of an upper-level isolated PV anomaly towards a surface baroclinic zone (sic. Rossby wave-guide). However the upper-level anomaly itself has usually either evolved from, or is located contiguous to, the upper-level Rossby wave-guide that is aligned along the extratropical

jet stream. Here consideration is given to the *dynamics* of localized PV anomalies and to the evolution of baroclinic systems in an idealized setting. Two complementary theoretical studies are undertaken of the nature of baroclinic development in the presence of all three-ingredients (i.e. two Rossby wave-guides and a PV anomaly). Emphasis is put on the sensitivity of the development to the scale, strength and location of the anomaly relative to the Rossby wave-guides. Section 2 deals with the standard two-dimensional linear Eady problem modified to include an interior vertically-localized PV distribution. In section 3 the non-linear evolution of a baroclinic jet is investigated under the influence of localized anomalies (boundary and interior) again in a Eady-like configuration.

## 2. THE STANDARD EADY SETTING

Interlevel interactions are considered in the traditional Eady model, consisted of a zonal flow of uniform stratification and a transverse thermal gradient (uniform baroclinic shear  $U = \Lambda z$ ). From a PV perspective the only dynamically important feature is the distribution of the perturbation potential temperature along the rigid upper and lower boundaries. The flow can be viewed as the co-development of two thermal baroclinic edge waves propagating on the pseudo PV gradient of potential temperature (Davies and Bishop, 1994, noted as DB) that are coupled by their velocity fields (interlevel interaction). For this configuration DB indicated the mechanisms of transient growth (the existence of maximal instantaneous thermal growth rates exceeding those of Eady NM) and that the long scale couplets asymptote towards the counterpart Eady NM.

Here the system is modified by introducing a PV wave with a biharmonic structure in the horizontal and a  $\delta$ -function vertical distribution at a stipulated level. This wave's thermal response vanishes on both boundaries and a set of equations can be derived that represents amplitude coupling and phase-speed modulation of the interacting boundary and PV waves. The strength of the coupling is related to the scale of the waves, to their amplitudes and relative phases and to the position of the PV anomaly.

The important parameters are the zonal wavenumber  $k$  of the waves, the vertical location  $h$  of the PV anomaly, the initial amplitudes and the initial relative phases  $\xi_T(0)$ ,  $\xi_B(0)$  between the

---

\*Corresponding author address: Sébastien Dirren, Swiss Federal Institute of Technology, Institute for Atmospheric Sciences, Hönggerberg HPP L6, 8093 Zurich, Switzerland, e-mail: sdirren@atmos.umnw.ethz.ch

PV and the surface waves (the subscripts T and B design respectively the top and the bottom of the domain). We choose typical values for the other parameters. The meridional wave number is taken to be  $l = \frac{1}{2}$  (6000 km wide channel). The pseudo-zonal wavenumber is such that  $k = (0.5, 1.5, 2.5)$  corresponds to wavelengths of (12000 km, 4000 km, 2400 km), the most unstable NM to  $k \simeq 1.55$  and the Eady cutoff to  $k_c \simeq 2.4$ .

For the triggering problem (surface  $B_{t=0} = 0$ ) the initial upper-level thermal and PV waves are assigned the same magnitude  $T_0 = T_{PV}$ .

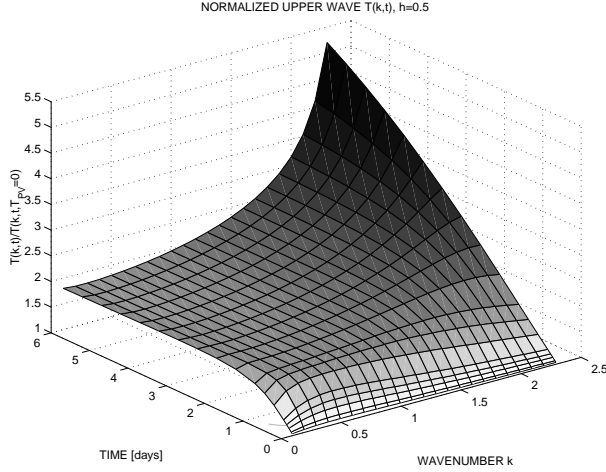


Figure 1: Time dependence of the amplitude of the upper-level wave  $T(k, t)$  on the zonal wavenumber. All values are normalized by the corresponding simulations with vanishing vortex anomaly ( $\frac{T}{T(T_{PV}=0)}$ ). The PV wave has a strong influence, especially on intermediate waves. Ultralong waves are less sensitive. The lower wave amplitude shows similar characteristics.

Consider the dependence of the time evolution of the amplitude  $T(k, t)$  of the upper wave on the zonal wavenumber  $k$  (for an anomaly localized in the middle of the domain). With time the maximum value shifts from  $k = 0.5$  (largest transient growth) to  $k = 1.5$  with different dependency to without PV anomaly (not shown). The maximum net development is reached for long waves ( $k < k_c$ ), whereas short waves ( $k > k_c$ ) show a very small development, because of a periodical time evolution beyond the Eady cutoff. Fig. 1 provides a comparison of the growth rate with that for the standard Eady setting (e.g.  $\frac{T(k,t)}{T(k,t,T_{PV}=0)}$ ). The anomaly has a significant effect upon intermediate waves ( $2 < k < k_c$ ) and substantial effect in the region of the most unstable NM (typical midlatitude cyclogenesis scales). Ultralong waves ( $k < 1$ ) are less sensitive to the PV waves than the intermediate ones.

Fig. 2 and 3 illustrate the influence of the PV wave in terms of vertical location and relative initial phase with the upper boundary temperature for  $k = 2$ , for respectively short and long time. In the former case maximal development on a boundary is reached for a PV anomaly localized in the vicinity

of that boundary. For longer time periods maximal development occurs for a PV wave localized near the middle of the domain, at the steering level. The sensitivity to vertical position of the anomaly is enhanced for shorter waves and reduced for longer waves.

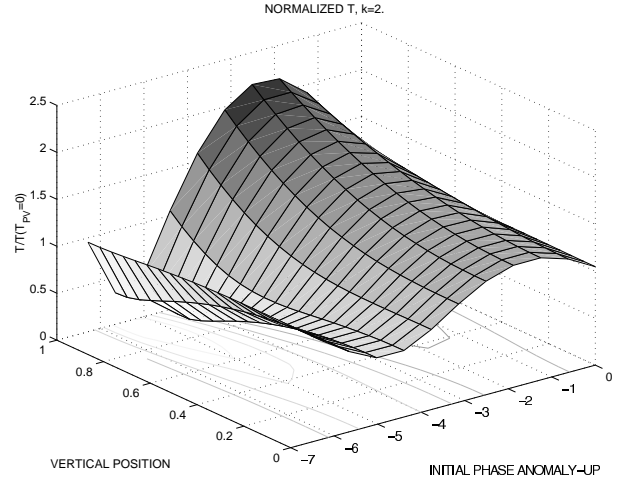


Figure 2: Short time (half a day) dependence of the normalized upper-level amplitude  $\frac{T}{T(T_{PV}=0)}(\xi_T, h)$  on the initial phase  $\xi_T$  between the anomaly and the upper-level and on the vertical position  $h$  of the anomaly. It shows maximal sensitivity for an anomaly localized near the upper boundary. The low-level amplitude shares similar characteristics, with maximal value when it is localized near the bottom of the model.

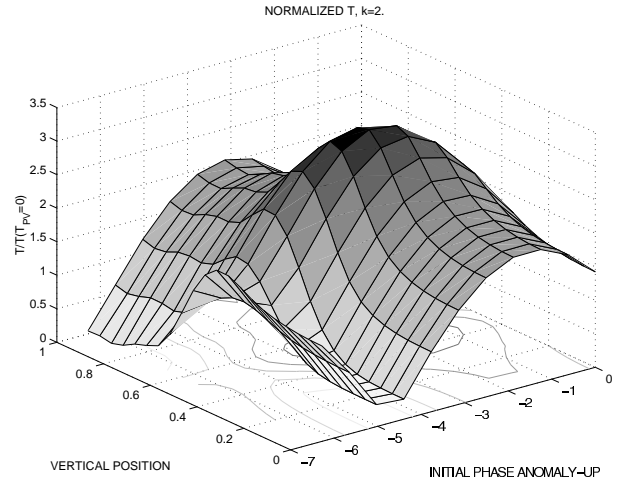


Figure 3: As Fig. 2, but for the longer time limit (6 days). Maximal effect is reached for an anomaly localized at the steering level.

These results can be interpreted in terms of two effects: the  $(k, h)$ -dependence of the couplings between the PV anomaly and the boundaries ( $\Delta_T(k, h)$ ,  $\Delta_B(k, h)$ ), and the phase modulations induced by these couplings. An anomaly near a boundary increases the coupling with that boundary

and enhances the in-situ development. However it decreases the coupling with the other boundary (in comparison with a PV at an intermediate vertical location) and therefore reduces the degree of mutual enhancement of the boundary waves. Shifting the anomaly away from the steering level allows the phase between the anomaly and the edge waves to oscillate in time, and limits the sustained growth. Hence after longer time periods, the optimal vertical location is at the steering level.

At a vertical location the PV wave and a thermal boundary wave can remain in phase (the resonance described in DB). For short waves the location for resonance lies in the same half of the domain as the boundary itself.

In summary PV waves can significantly invigorate the development, especially in the case of intermediate-scale waves. For short periods of time maximal effect is on the top (bottom) for a wave localized on the top (bottom) and the anomaly strongly reinforces the boundary wave. Over longer time periods, maximal effect is for a PV wave located in the middle of the domain.

### 3. THE EXTENDED EADY SETTING

A non-linear channel model is used in the idealized framework of the adiabatic quasi-geostrophic dynamics of a uniform PV atmosphere on a  $f$ -plane for a jetlike baroclinic flow sandwiched between two rigid vertical boundaries. The basic state is characterized by a two-dimensional symmetric baroclinic zone, a region with a temperature contrast of  $18^\circ$  K and a width of 4000 km balanced by a zonal jet in upper troposphere (30 m/s).

First experiments are performed to study the influence of the latitudinal position of an initial non-modal thermal anomaly upon upper-level-induced cyclogenesis. Then the influence of an interior point-vortex anomaly is investigated.

The selection of a norm is an open issue in non-modal studies. From a meteorological standpoint values of the surface pressure are of interest. From a dynamical standpoint less localized norms (e.g. the sum of the potential temperature/energy perturbations on each boundary) is meaningful since all the dynamics is determined on the boundaries. For the setting with an interior vortex we adopt a pragmatic approach : the vortex's amplitude is set by the velocity signature at the upper boundary.

#### 3.1 TROPOPAUSE-LEVEL ANOMALY (no interior vortex)

The initial perturbation consists of a thermal anomaly at the top (Pettersson type B cyclogenesis) and we examine this response as a function of the anomaly's location relative to the baroclinic zone.

Figure 4 shows the mean growth rate (over 6 days) of the extrema of pressure perturbation at the bottom of the domain, for a specified initial anomaly. Also shown is the growth that is expected from the linear evolution of the most unstable NM (dashed

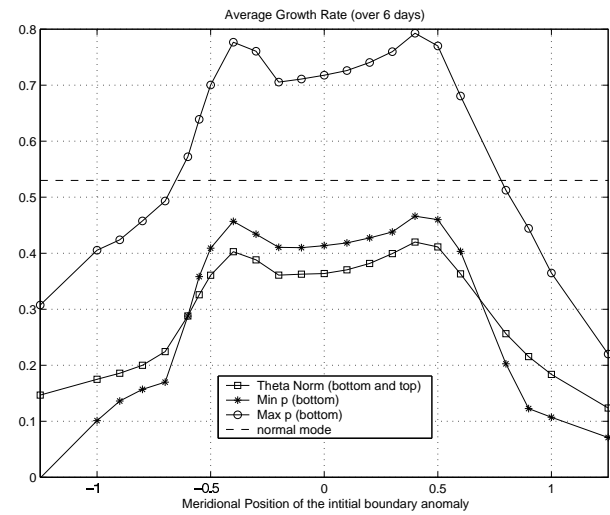


Figure 4: Mean growth rates (over 6 days) of the maximum and minimum pressure perturbation (bottom) and of the sum of the  $\theta$ -perturbation (top-bottom) as function of the meridional initial position of the upper-level thermal anomaly (radius  $r=200km$ ). Positive values in the x-axis point to the south (warm region).

line). The growth rates decrease when the perturbation is outside the baroclinic zone, but display two peaks. Indeed the growth rates are higher than those corresponding to a central initial anomaly. This sustained growth is linked to the relative constancy of the phase between the anomaly and the most unstable linear NM (time independent for an anomaly being advected along the critical lines).

In summary the maximum pressure at the bottom grows faster than the most unstable NM during the first two days, with a maximum growth for the central anomaly. After this transient period it grows at a rate close to that of the NM, whereas the rates are bigger for an anomaly being advected along the critical lines.

#### 3.2 INTERIOR TROPOSPHERIC ANOMALY

Now the initial configuration consists of an interior anomaly, which is such that its thermal signal at the boundaries vanish. Its strength is set by the velocity field that it induces on the boundaries.

For short periods, the maximal growth at one boundary is obtained with a vortex localized near that boundary (in comparison to the development reached by a mid-level height vortex). For longer time intervals this favourable development on one boundary will be offset by the lack of development on the other. Moreover after a period of sustained growth we have a period of strong destructive interferences, due to a varying phase for an anomaly localized far from the steering level.

#### 3.3 VORTEX AND BOUNDARY ANOMALIES

Now we initialize the model with both the thermal and the vortex anomalies. The dependence on the vertical position of the vortex is similar to that for the vortex alone. Fig. 5 attests that the presence of

the vortex ensures a more favourable development (compared with the no-vortex experiment).

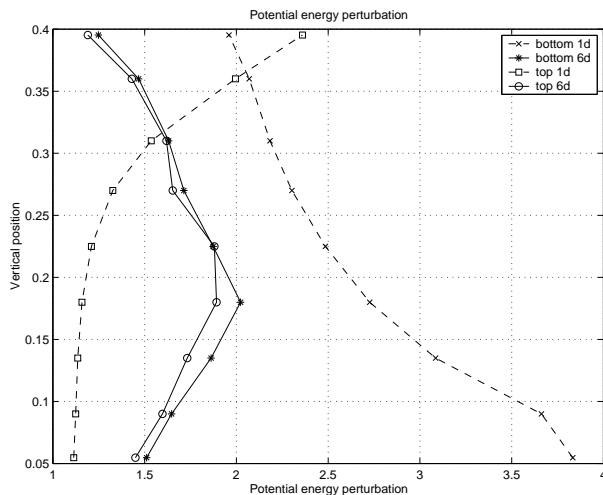


Figure 5: Dependence of the sum of the perturbation potential energy (at the top and bottom, x-axis) on the vertical position (y-axis) of the vortex anomaly (normalized by the corresponding value of the simulations without vortex) and for short (1 day, dashed) and long (6 days) time. The steering level is at 0.18, the top of the domain at 0.45.

For a low-level vortex there is a stronger development at the bottom and a slightly weaker one at the top compared with that for a vortex located at  $h = 0.18$  (but always stronger than the no-vortex experiment). Over a short period of time, the growth rates at the bottom are more pronounced, but this is not valid later. Similar results apply for an upper-level vortex.

#### 4. FURTHER REMARKS

We have discussed the nature of the response to an interior anomaly from a physical and dynamical standpoint. It yields similar results as those presented in Fig. 4 for an initial upper-level boundary potential temperature anomaly. The large transient growth rates encountered in the first stage of the evolution create very rapidly a finite-amplitude effect which is important and needs specific consideration.

The results give some indication that the tropopause level is strongly sensitive to the relative positions of interior and boundary anomalies. The presence of *finite amplitude* structures at upper-levels can play an important role in triggering the cyclogenesis, and the interaction of localized PV elements at upper-levels can modify the subsequent interlevel co-development (Fehlmann and Davies, 1997).

#### REFERENCES

Badger, J. and B.J. Hoskins, 2000: Simple initial Value Problems and Mechanisms for Baroclinic Growth, *J. Atmos. Sci.*, revised.

Davies, H. C and C.H. Bishop, 1994: Eady Edge Waves and Rapid Development, *J. Atmos. Sci.*, **51**, 1930–1946.

Farrell, B.F. The initial Growth of Disturbances in baroclinic Flows, *J. Atmos. Sci.*, **39**, 1963–1986.

Fehlmann, R. and H.C. Davies, 1997: Misforecasts of Synoptic Systems: Diagnosis via PV Retrodiction, *Mon. Wea. Rev.*, **125**, 2247–2264.

Hoskins, B.J., R. Buizza and J. Badger, 2000: The Nature of Singular Vector Growth and Structure, *Q.J.R.Meteorol.Soc.*, **126**

Hoskins, B.J. and N.V. West, 1979: Baroclinic waves and frontogenesis. Part II: uniform potential vorticity jet flows, *J. Atmos. Sci.*, **36**, 1663–1680.

Molteni, F., R. Buizza, T.N. Palmer and T. Petroliagis, 1996: The ECMWF Ensemble Prediction System : Methodology and Validation, *Q.J.R.Meteorol.Soc.*, **122**, 73–119.

Morgan, M.C., 2000: A Potential Vorticity and Wave Activity Diagnosis of Optimal Perturbation Evolution, *J. Atmos. Sci.*, submitted.